

Information flow in a network model and the law of diminishing marginal returns

D. Marinazzo,¹ M. Pellicoro,² Guo-Rong Wu,^{1,3} L. Angelini,² and S. Stramaglia²

¹*Faculty of Psychology and Educational Sciences, Department of Data Analysis,
Ghent University, Henri Dunantlaan 1, B-9000 Ghent, Belgium*

²*Dipartimento di Fisica, Università degli Studi di Bari and INFN, via Orabona 4, 70126 Bari, Italy*

³*Key Laboratory for NeuroInformation of Ministry of Education, School of Life Science and Technology,
University of Electronic Science and Technology of China, Chengdu 610054, China*

(ΩDated: January 10, 2019)

We analyze a simple dynamical network model which describes the limited capacity of nodes to process the input information. For a suitable choice of the parameters, the information flow pattern is characterized by exponential distribution of the incoming information and a fat-tailed distribution of the outgoing information, as a signature of the law of diminishing marginal returns. The analysis of a real EEG data-set shows that similar phenomena may be relevant for brain signals.

PACS numbers: 05.10.-a, 05.45.Tp, 87.18.Sn

Most social, biological, and technological systems can be modeled as complex networks, and display substantial non-trivial topological features [1, 2]. Moreover, time series of simultaneously recorded variables are available in many fields of science; the inference of the underlying network structure, from these time series, is an important problem that received great attention in the last years. A method based on chaotic synchronization has been proposed in [3], a method rooted on L1 minimization has been described in [4]. Use of a phase slope index to detect directionalities of interactions has been proposed in [5]. The inference of dynamical networks is also related to the estimation, from data, of the flow of information between variables. The information flow between variables is measured by the transfer entropy [6, 7], which captures the dynamics by means of rates of entropy change. On the other hand, Wiener [8] and Granger [9] formalized the notion that, if the prediction of one time series could be improved by incorporating the knowledge of past values of a second one, then the latter is said to have a *causal* influence on the former. Initially developed for econometric applications, Granger causality has gained popularity also among physicists (see, e.g., [10–15]) and eventually became one of the methods of choice to study brain connectivity in neuroscience [16]. Multivariate Granger causality may be used to infer the structure of dynamical networks from data as described in [17]. It has been recently shown that, for Gaussian variables, Granger causality and transfer entropy are equivalent [18]. Hence, at least for linear systems, Granger causality provides a weighted network with a rigorous interpretation in terms of flow of information between different components of a system. This way to look at information flow is particularly relevant for neuroscience, where it is crucial to shed light on the communication among neuronal populations, which is the mechanism underlying the information processing in the brain. This framework represents a bridge between effective connectivity, which can be inferred from the parameters of a model (such as

in Granger causality or dynamic causal modeling), or to directed functional connectivity, assessed by model-free methods such as transfer entropy [19].

In many situations it can be expected that each node of the network may handle a limited amount of information. This structural constraint suggests that information flow networks should exhibit some topological evidences of the law of diminishing marginal returns [20], a fundamental principle of economics which states that when the amount of a variable resource is increased, while other resources are kept fixed, the resulting change in the output will eventually diminish [21, 22]. The purpose of this work is to introduce a simple dynamical network model where the topology of connections, assumed to be undirected, gives rise to a peculiar pattern of the information flow between nodes: a fat tailed distribution of the outgoing information flows while the average incoming information flow does not depend on the connectivity of the node. We then show that this relevant topological feature is found as well in real neural data.

Our model is as follows. Given an undirected network of n nodes and symmetric connectivity matrix $A_{ij} \in \{0, 1\}$, to each node we associate a real variable x_i whose evolution, at discrete times, is given by:

$$x_i(t+1) = F\left(\sum_{j=1}^n A_{ij}x_j(t)\right) + \sigma\xi_i(t), \quad (1)$$

where ξ are unit variance Gaussian noise terms, whose strength is controlled by σ ; F is a transfer function chosen as follows:

$$\begin{aligned} F(\alpha) &= a\alpha & |\alpha| < \theta \\ F(\alpha) &= a\theta & \alpha > \theta \\ F(\alpha) &= -a\theta & \alpha < -\theta \end{aligned} \quad (2)$$

where θ is a threshold value. This transfer function is chosen to mimic the fact that each unit is capable to handle a limited amount of information. For large θ our model becomes a linear map. At intermediate values of

θ , the nonlinearity connected to the threshold will affect mainly the mostly connected nodes (hubs). We consider hierarchical networks generated by preferential attachment mechanism [23]. From numerical simulations of eqs. (1), we evaluate the linear causality pattern for this system as the threshold is varied. We verify that, in spite of the threshold, variables are nearly Gaussian so that we may identify the causality with the information flow between variables [18]. We compute the incoming and outgoing information flow from and to each node, c_{in} and c_{out} , summing respectively all the sources for a given target and all the targets for a given source. Then we evaluate the standard deviation of c_{in} and c_{out} over the nodes of 100 realizations of preferential attachment networks, each with 10 simulations of eqs. (1) for 10000 points.

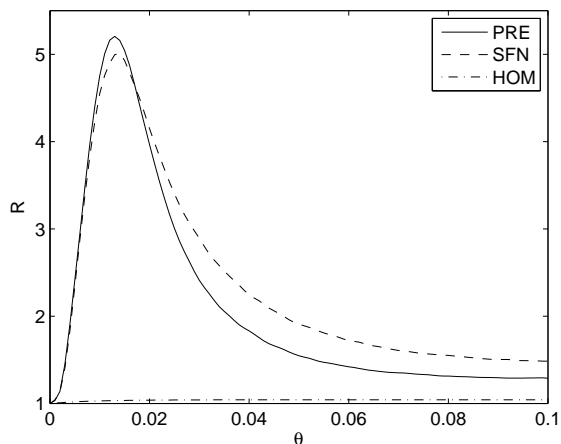


FIG. 1: The ratio between the standard deviation of c_{out} and those of c_{in} , R , is plotted versus θ for the three architectures of network: preferential attachment (PRE), deterministic scale free (SFN) and homogeneous (HOM). The parameters of the dynamical system are $a = 0.1$ and $s = 0.1$. Networks built by preferential attachment are made of 30 nodes and 30 undirected links, while the deterministic scale free network of 27 nodes is considered. The homogeneous networks have 27 nodes, each connected to two other randomly chosen nodes.

In figure (1) we depict R , the ratio between the standard deviation of c_{out} over those of c_{in} , as a function of the θ . As the threshold is varied, we encounter a range of for which the distribution of c_{in} is much narrower than that of c_{out} . In the same figure we also depict the corresponding curve for deterministic scale free networks [24], which exhibits a similar peak, and for homogeneous random graphs (or Erdos-Renyi networks [25]), with R always very close to one. The discrepancy between the distributions of the incoming and outgoing causalities arises thus in hierarchical networks. We remark that, in order to quantify the difference between the distributions of c_{in} and c_{out} , here we use the ratio of standard deviations but

qualitatively similar results would have been shown using other measures of discrepancy.

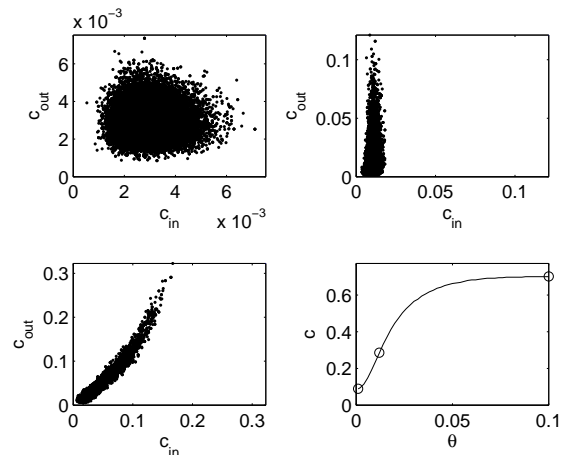


FIG. 2: Scatter plot in the plane $c_{in} - c_{out}$ for undirected networks of 30 nodes and 30 links built by means of the preferential attachment mechanism. The parameters of the dynamical system are $a = 0.1$ and $s = 0.1$. (Top-left) Contour plot of the distribution for all nodes at $\theta = 0.001$. (Top-right) Contour plot of the distribution for all nodes at $\theta = 0.012$. (Bottom-left) Contour plot of the distribution for all nodes at $\theta = 0.1$. (Bottom-right) The total causality (obtained summing over all pairs of nodes) is plotted versus θ ; circles point to the values of θ in the previous subfigures.

In (2) we report the scatter plot in the plane $c_{in} - c_{out}$ for preferential attachment networks and for some values of the threshold. The distributions of c_{in} and c_{out} , with θ equal to 0.012 and corresponding to the peak of fig. (1), are depicted in fig. (3): c_{in} appears to be exponentially distributed around a typical value, whilst c_{out} shows a fat tail. In other words, the power law connectivity of the network influences just the distribution of outgoing causalities.

In fig. (4) we show the average value of c_{in} and c_{out} versus the connectivity k of the network node: c_{out} grows uniformly with k , thus confirming that its fat tail is a consequence of the power law of the connectivity. On the contrary c_{in} appears to be almost constant: on average the nodes receive the same amount of information, irrespectively of k , whilst the outgoing information from each node depends on the number of neighbors.

It is worth mentioning that since a precise estimation of the information flow is computationally expensive, our simulations are restricted to rather small networks; in particular the distribution of c_{out} appears to have a fat tail but, due to our limited data, we can not claim that it corresponds to a simple power-law.

In fig. (5) the distributions of c_{in} and c_{out} are depicted for nodes of connectivity 8. Given the connectivity of a node, the values of c_{in} and c_{out} are almost exactly determined, the uncertainty being due to variability in

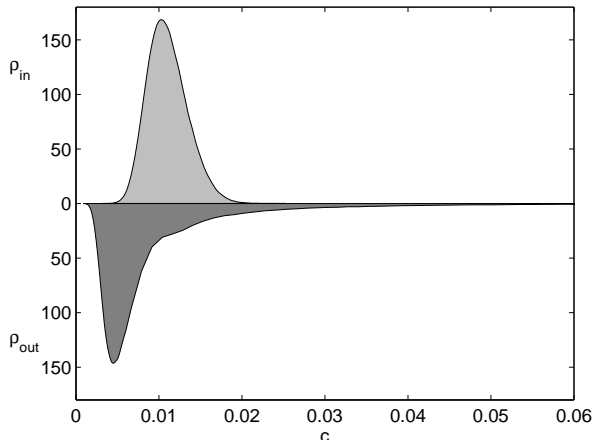


FIG. 3: For the preferential attachment network, at $\theta = 0.012$, the distributions of c_{in} and c_{out} are depicted. Units on the vertical axis are arbitrary.

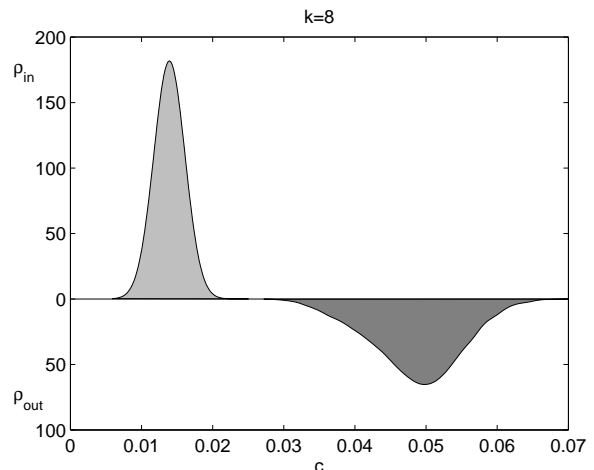


FIG. 5: For the preferential attachment network, at $\theta = 0.012$, the distributions of c_{in} and c_{out} are depicted for the nodes with connectivity equal to 8. Units on the vertical axis are arbitrary.

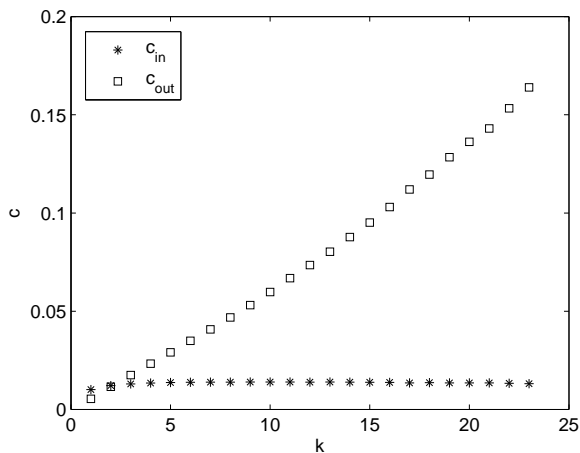


FIG. 4: For the preferential attachment network, at $\theta = 0.012$ the average c_{in} and c_{out} is plotted versus the connectivity of the node.

the realization of the preferential attachment network.

Now we turn to consider real electroencephalogram (EEG) data. We used recording obtained at rest from 10 healthy subjects. During the experiment, which lasted for 15 min, the subjects were instructed to relax and keep their eyes closed. Every minute the subjects were asked to open their eyes for 5 s. EEG was measured with a standard 10-20 system consisting of 19 channels [5]. Data were analyzed using the linked mastoids reference, and are available from [26].

For each subject we considered several epochs of 4 seconds. For each epoch we computed multivariate Kernel Granger Causality [15] using a linear kernel and a model order of 5, determined by leave-one-out cross-validation. We then pooled all the values for information flow to-

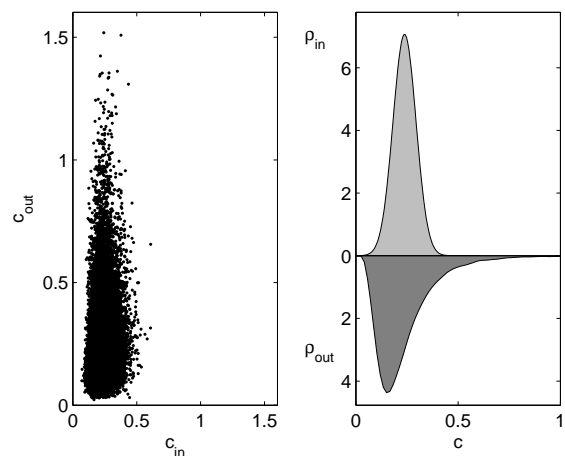


FIG. 6: For the EEG data the distributions of c_{in} and c_{out} are depicted in a scatter plot (left) and in terms of their distributions (right).

wards and from any electrode and analyzed their distribution.

In figure (6) we plot the incoming versus the outgoing values of the information flow, as well as the distributions of the two quantities: the incoming information seems exponentially distributed whilst the outgoing information shows a fat tail. These results suggest that brain effective connectivity networks may also be considered in the light of the law of diminishing marginal returns. It is worthwhile to mention that we verify that also other measures of directed brain connectivity, such as Directed Transfer Function, Partial Directed Coherence and Phase Slope Index resulted in distributions which are qualitatively similar; nonetheless for DTF and PDC, defined in

terms of physiological bands, we cannot speak exactly of information transfer because the relation between transfer entropy and Granger causality does not hold for spectral Granger causality. Furthermore, bivariate measures do not display this asymmetry of the distributions of c_{in} and c_{out} : this is not surprising, indeed it is well known that bivariate causality also account for indirect interactions, see e.g. [17]. Here we limited ourselves to linear information flow; the amount of nonlinear information transmission and its functional roles are not clear [27]. It will be interesting to investigate these phenomena also in the nonlinear case.

Summarizing, we have pointed out that the pattern of information flows among variables of a complex system is the result of the interplay between the topology of the underlying network and the capacity of nodes to handle the incoming information. By means of a simple toy model, we have shown that it may exhibit the law of diminishing marginal returns for a suitable choice of parameters. The analysis of a real EEG data-set has shown that similar patterns may apply for brain signals; these phenomena may be relevant for the functioning of neural systems.

-
- [1] A.L. Barabasi, *Linked: the new science of networks*. (Perseus Publishing, Cambridge Mass., 2002)
- [2] S. Boccaletti, V. Latora, Y. Moreno, M. Chavez and D.-U. Hwang, *Phys. Rep.* **424**, 175 (2006)
- [3] D. Yu, M. Righero, L. Kocarev, *Phys.Rev.Lett.* **97**, 188701 (2006).
- [4] D. Napoletani, T. Sauer, *Phys. Rev.* **E 77**, 26103 (2008)
- [5] G. Nolte, A. Ziehe, V. Nikulin, A. Schlögl, N. Krämer, T. Brismar, K.R. Müller, *Phys. Rev. Lett.* **100**, 234101, 2008
- [6] T. Schreiber, *Phys. Rev. Lett.* **85**, 461 (2000)
- [7] M. Staniek, K. Lehnertz, *Phys. Rev. Lett.* **100**, 158101 (2008)
- [8] N. Wiener, *The theory of prediction*. In E.F. Beckenbach, Ed., *Modern mathematics for Engineers*. (McGraw-Hill, New York, 1956)
- [9] C.W.J. Granger, *Econometrica* **37**, 424 (1969)
- [10] J. Geweke, *J. Am. Stat. Assoc.* **79**, 907 (1984)
- [11] Y. Chen, G. Rangarajan, J. Feng and M. Ding, *Phys. Lett. A* **324**, 26 (2004)
- [12] K.J. Blinowska, R. Kus, M. Kaminski, *Phys. Rev. E* **70**, 50902(R) (2004)
- [13] D.A. Smirnov, B.P. Bezruchko, *Phys Rev.* **E 79**, 46204 (2009)
- [14] M. Dhamala, G. Rangarajan, M. Ding, *Phys. Rev. Lett.* **100**, 18701 (2008)
- [15] D. Marinazzo, M. Pellicoro, S. Stramaglia, *Phys. Rev. Lett.* **100**, 144103 (2008)
- [16] S.L. Bressler, A.K. Seth, *Neuroimage* **58** 323 (2011)
- [17] D. Marinazzo, M. Pellicoro and S. Stramaglia, *Phys. Rev. E* **77**, 056215 (2008)
- [18] L. Barnett, A.B. Barrett, and A.K. Seth, *Phys Rev. Lett.* **103**, 238701 (2009)
- [19] K.J. Friston, *Brain connectivity* **1**, 13 (2011)
- [20] P. Samuelson, W. Nordhaus, *Microeconomics*, Mc Graw Hill, Edition 17 (2001)
- [21] L. Lopez, M.A.F. Sanjuan, *Phys. Rev. E* **65** 036107 (2002)
- [22] J. A. Almendral,, L. Lopez, M. A. F. Sanjuan, *Physica A* **324**, 424 (2003)
- [23] Barabasi, A.-L.; R. Albert, *Science* **286** 509512 (1999)
- [24] A.-L. Barabasi, E. Ravasz and T. Vicsek, *Physica A* **299**, 559-564 (2001)
- [25] P. Erdős and A. Rényi, *Publ. Math. Inst. Hung. Acad. Sci.* **5**, 17 (1960)
- [26] <http://clopinet.com/causality/data/nolte/>, accessed february 2012
- [27] D. Marinazzo, W. Liao, H. Chen, S. Stramaglia, *Neuroimage* **58**, 330 (2011)